Green CO_2 from Oxy-Steam Combustion of Biogenic Fuels

Hannah Cortnum[a], Maximilian Weitzer[a] and Jürgen Karl[a]

[a] Chair of Energy Process Engineering, Friedrich-Alexander-Universität Erlangen-Nürnberg (FAU), Nürnberg, Germany
Corresponding author: hannah.cortnum@fau.de

Abstract:

The defossilization of the process heating and transportation sectors requires integration with the electricity system through Power-to-X technologies. Alongside hydrogen generated by water electrolysis, carbon dioxide (CO_2) is necessary as a carbon source for synthetic renewable fuels and gases. Additionally, CO_2 is widely used for fertilization in commercial horticulture. Oxyfuel combustion of biogenic solid fuels produces a CO_2- and water-rich flue gas from which green CO_2 can be provided by condensation. The condensation heat can be utilized for greenhouse heating. The oxygen required for oxyfuel combustion is provided as a by-product of water electrolysis. Conventional oxyfuel technologies require flue gas recirculation to moderate the high combustion temperatures, which increases system complexity and electrical power demand. Oxy-steam combustion represents an alternative approach in which temperature control is achieved by recirculation of the aqueous condensate from a flue gas condenser instead of the CO_2-rich flue gas. In this work, thermodynamic process simulations investigate three cooling strategies for a bubbling fluidized bed during oxy-steam operation and compare the oxy-steam combustion with conventional oxyfuel combustion with wet and dry flue gas recirculation. The results indicate that oxy-steam combustion achieves thermal efficiencies comparable to conventional oxyfuel concepts while requiring significantly lower electrical power due to the replacement of the recirculation fan by a condensate pump. To demonstrate the CO_2 provision by oxy-steam combustion experimentally, a laboratory-scale fluidized bed combustion system is being retrofitted for oxy-steam operation. This includes the integration of steam and oxygen supply, a flue gas cooler and a direct contact condenser.

Keywords:

oxyfuel combustion; oxy-steam combustion; fluidized bed; BECCUS; biogenic fuels.

1. Introduction

The ongoing defossilization of the process heating and transportation sectors and the chemical industry depends on their integration with the electricity system via Power-to-X (PtX) technologies. Alongside hydrogen generated by water electrolysis, carbon dioxide (CO_2) is necessary as a carbon source for synthetic fuels and gases and renewable platform chemicals [1]. When CO_2 is supplied from bioenergy, net-zero emissions can be achieved or, if the CO_2 is permanently stored, negative emissions are possible. This concept is referred to as “bioenergy with carbon capture, utilization and storage” (BECCUS) [2, 3]. It represents an extension of the concept “bioenergy with carbon capture and storage” (BECCS) introduced by [4]. During photosynthesis, atmospheric CO_2 is captured and fixated in biomass. The biomass is then used energetically, e.g., through combustion, and the resulting CO_2 emissions can be captured to prevent their release into the atmosphere [3].

In addition to PtX applications, CO_2 is also required for greenhouse fertilization. Optimal crop growth occurs at around 1000 ppm, far above ambient levels of 350-450 ppm. Without supplementation, CO_2 in the greenhouse can drop below ambient due to plant uptake, so maintaining even ambient levels would require substantial ventilation. CO_2 is typically supplied from the flue gas of natural gas or propane boilers, or via liquid CO_2. Liquid CO_2 is often preferred for its purity, though it is more expensive, while natural gas boilers can also provide integrated heat supply [5, 6]. Li et al. [7] and Dion et al. [8] reviewed different renewable sources for CO_2 enrichment in greenhouses including biomass heating systems.

Another renewable approach to CO_2 fertilization is the use of oxyfuel combustion of biogenic solid fuels. Oxyfuel combustion provides a flue gas consisting mainly of water and CO_2, from which CO_2 can be easily separated by condensation. Also, the system´s condensation heat can be used for greenhouse heating. The technologies most commonly applied to solid fuels in oxyfuel combustion are pulverized fuel combustion and circulating fluidized bed (CFB) systems [9, 10]. Fluidized bed reactors are advantageous for biomass combustion due to their fuel flexibility in terms of ash and moisture content. Additionally, good gas-solid mixing prevents local overheating, which reduces emissions and the risk of ash melting [9, 11]. So far, pilot scale

demonstrations (> 100 kW_{th}) of oxyfuel combustion of biomass have mainly focused on co-combustion mode to reduce greenhouse emissions from coal power plants. CIUDEN in Spain demonstrated oxyfuel co-combustion in a 30 MW_{th} CFB boiler, the world´s largest oxyfuel CFB plant, commissioned in 2011 [10, 12]. Kuhn et al. [13] studied the oxyfuel combustion of solid recovered fuels in a 1 MW_{th} CFB reactor and plan to examine biomass fuels in future studies. CanmetEnergy in Canada co-fired 20-50 wt% biomass in a 0.8 MW_{th} CFB reactor and found that adding biomass did not significantly change the combustion characteristics [14]. On a laboratory scale (< 100 kW_{th}), CIRCE in Spain demonstrated oxyfuel co-combustion in a bubbling fluidized bed (BFB) reactor that operated at up to 70 kW_{th} [15, 16]. The oxyfuel combustion of pure biomass fuels including various types of wood, rice husk, straw and sewage sludge was conducted in CFB reactors by [17–22], with a focus on pollutant emissions, oxygen-carrier aided combustion, and pressurized oxyfuel combustion. Sher et al. [23] investigated the oxyfuel combustion of pure biomass in a 20 kW_{th} BFB reactor focusing on the influence of the combustion atmosphere on the emissions. Vodička et al. [24] studied a 30 kW_{th} BFB reactor and analyzed the use of a lightweight ceramic aggregate as bed material.

The challenges of oxyfuel combustion include the high temperatures in a pure oxygen (O_2) atmosphere due to the absence of the inert nitrogen in the air. In conventional oxyfuel combustion, these high temperatures are moderated by recirculation of the flue gas. Typically, 60-80 vol% of the flue gas are recycled back to the combustion chamber. The flue gas recirculation (FGR) can be classified as either dry or wet. Dry recirculation occurs after flue gas condensation, while wet recirculation before flue gas condensation [9]. The FGR fan and, in particular, the air separation unit, which consumes up to 30 % of the electricity generated in oxyfuel power plants to provide pure oxygen, increase the electrical power demand of oxyfuel combustion plants [9, 25].

To avoid flue gas recirculation, the alternative oxyfuel concept oxy-steam combustion has been proposed. Instead of recirculating the flue gas for temperature moderation, the aqueous condensate from the flue gas condenser is recycled back to the combustion chamber in form of steam or liquid. Replacing the recirculation fan with a pump lowers the electricity demand and reduces the size of the recirculation system [25]. The oxy-steam combustion concept was introduced by CanmetEnergy in 2007 as a 3rd generation oxyfuel combustion system to avoid flue gas recirculation and a prototype pulverized coal burner was designed for various operation modes [26]. In 2008, Seepana and Jayanti filed a patent for the “steam-moderated oxy-fuel combustion” process and conducted a flame structure analysis and thermodynamic exergy analysis for comparison with air combustion [27]. Several authors mainly studied the combustion characteristics, such as ignition behavior, flame characteristics, char combustion, and NO_x formation, within single particle experiments, which were reviewed by [28]. Sheng et al. [29] and Jin et al. [25] conducted process simulations to compare oxy-steam combustion with conventional oxyfuel combustion in power plants. They found that the two processes reach comparable energy and exergy efficiencies. Studies on oxy-steam combustion of biomass in larger laboratory scale units are limited. Moroń et al. [30] studied the oxy-fuel combustion of biomass with up to 10 % steam in an entrained flow reactor and found that SO_2 and NO_x emissions are slightly reduced by addition of steam. Lu et al. [31] tested biomass oxyfuel combustion in an entrained flow reactor with up to 15 % steam addition and found that NO reduction was maximized at 2-6 % water vapor. Escudero et al. [32] and Díez et al. [33] studied the co-combustion of coal and biomass with up to 20 % biomass in a $O_2/CO_2/H_2O$ atmosphere with up to 40 % steam in a laboratory scale entrained flow reactor. They found that an optimal CO_2/H_2O ratio minimizes NO formation.

This study analyzes the supply of green CO_2 through the oxy-steam combustion of solid biogenic fuels using thermodynamic process simulations. Different concepts for condensate recirculation are discussed and the oxy-steam combustion is compared with conventional oxyfuel combustion employing dry and wet FGR. The oxygen required for oxyfuel combustion is assumed to be supplied as a by-product of water electrolysis, while the condensation heat of the process can be used to supply a heating network. In addition, the study presents the retrofitting of a laboratory scale BFB reactor for the future demonstration of oxy-steam combustion of biomass with a thermal input of 10-20 kW_{th}.

2. Setup of the Simulation Model

To study the oxy-steam combustion with condensate recirculation of different biogenic solid fuels and compare it to conventional oxyfuel combustion with FGR, a stationary model was setup with the software IPSEpro 8.0 by SimTech [34]. IPSEpro enables thermodynamic process simulations by solving energy and mass balances. Component models are created and modified within the Model Development Kit to build a library. On the process level, components are connected within the Process Simulation Environment and the Newton-Raphson method is applied for the numerical solution [35].

Figure 1 presents the process flow sheet in IPSEpro. The process starts with a proton exchange membrane (PEM) electrolyzer which provides oxygen for the oxyfuel combustion as a by-product of hydrogen production from water. The oxyfuel combustion takes place in a BFB combustion chamber. The combustion chamber is split into a primary combustion chamber, which acts as the fluidized bed, and a secondary combustion chamber, which represents the freeboard. This setup allows for the simplified simulation of a staged combustion process. As fluidization and primary oxidizing medium, a mixture of steam and oxygen is fed into

the fluidized bed together with biomass as fuel resulting in an oxy-steam combustion process. The flue gas and the secondary steam/O_2-mixture enter the secondary chamber. As a second cooling measure, liquid recirculated condensate can be introduced to the combustion chambers. The flue gas is cooled down by generating steam and enters the partial condenser. The partial condenser provides heat to a heating network. A portion of the resulting condensate is recirculated to the combustion process as liquid condensate and steam. The resulting flue gas consists now mainly of CO_2.

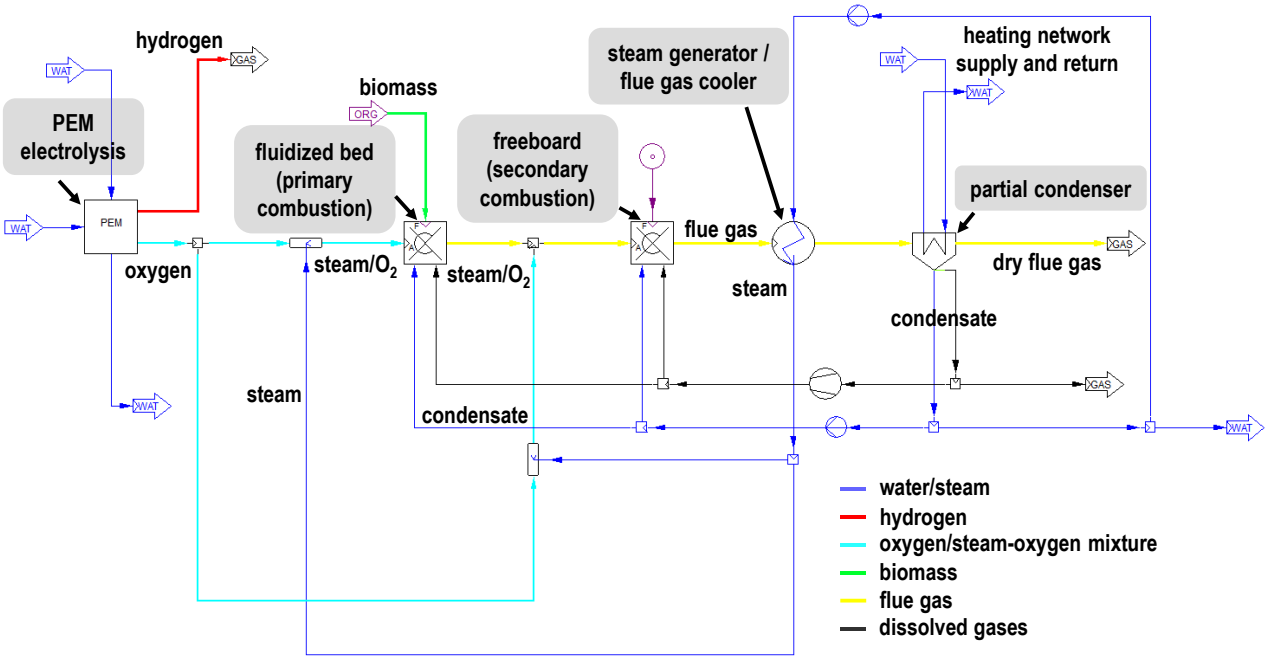

Figure 1. *Setup of the oxy-steam combustion simulation model with the software IPSEpro 8.0 [34].*

The PEM electrolyzer model calculates the efficiency, electrical energy input and mass flows based on technical input parameters [36]. The PEM model uses the polarization curve (current density (i)-voltage (U) characteristic) according to [37], a PEM nominal power $P_{el,nom}$ of 25 MW and a nominal current density i_{nom} of 2 A/cm^{-2} [38, 39]. Equations (1)-(3) are applied together with mass and energy balances to calculate the electrical power P_{el} and efficiency η_{PEM} [36, 38]. Mass balances are solved at the chemical element level because chemical reactions occur.

$$\eta_{PEM} = \frac{LHV_{mol,H2} \cdot \dot{n}_{H2}}{P_{el}} = \frac{LHV_{mol,H2}}{F \cdot U} \quad (1)$$

$$P_{el} = i \cdot U(i) \cdot A_{PEM} \quad (2)$$

$$A_{PEM} = i_{nom} \cdot U(i_{nom}) \cdot P_{el,nom} \quad (3)$$

In the combustion chamber models, mass and energy balances as well as combustion calculations are applied. Complete combustion converts the fuel entirely to CO_2, H_2O, N_2, SO_2 and HCl. In the case of incomplete combustion, hydrocarbons are not considered in the flue gas, the only incomplete oxidation product is CO [35]. In oxyfuel combustion, the conventional air-excess ratio is replaced by the oxygen-excess ratio λ, defined as the ratio of the supplied oxygen mass flow to the minimum oxygen demand required for complete combustion (Eq. (4)). The minimum oxygen demand is determined by the elemental composition of the fuel [40]. In the primary chamber (fluidized bed), substoichiometric conditions are assumed ($\lambda_{prim} < 1$). The available oxygen is assumed to react completely, leaving zero oxygen in the outlet gas ($w_{O_2,out,prim} = 0$). Due to oxygen deficiency, part of the fuel's carbon remains in the outlet gas as CO. This relationship is described by Eq. (5). In the secondary chamber, additional oxygen is supplied to achieve a global oxygen-excess ratio of at least 1 ($\lambda_{global} \geq 1$). The remaining CO formed in the primary chamber is assumed to be fully oxidized to CO_2. The amount of oxygen supplied to the secondary chamber is determined such that the global oxygen-excess ratio is achieved (Eq. (6)). The mass flows entering the combustion chambers are described by $\dot{m}_{in,sec}$ and $\dot{m}_{in,prim}$. The terms $w_{O_2,in,sec}$ and $w_{O_2,mix}$ denote the oxygen mass fractions of the secondary inlet stream and the steam/O_2-mixture. The oxygen fraction of the steam/O_2-mixture $w_{O_2,mix}$ is same for both combustion chambers.

As fuel, the simulations consider natural wood with no or insignificant amounts of bark, leaves or needle according to [41] and tomato greenhouse crop residues according to [42] with varying water content. The lower heating value (LHV) is calculated using Boie's formula [43].

$$\lambda = \frac{\dot{m}_{O_2}}{\dot{m}_{O_2,min}} \tag{4}$$

$$\lambda_{prim} \cdot \dot{m}_{out,prim} \cdot \left(w_{O_2,out,prim} - w_{CO,out,prim} \cdot \frac{M_{O_2}}{2M_{CO}} \right) = \dot{m}_{in,prim} \cdot w_{O_2,mix} \cdot (\lambda_{prim} - 1) \tag{5}$$

$$\dot{m}_{in,sec} \cdot w_{O_2,in,sec} = \dot{m}_{in,prim} \cdot w_{O_2,mix} \cdot \frac{\lambda_{global} - \lambda_{prim}}{\lambda_{prim}} \tag{6}$$

The flue gas condenser separates the water fraction from the gaseous components, mainly CO_2, in the flue gas. Since the condensate leaves the condenser in liquid form and the CO_2-rich gas leaves in gaseous form, the condenser functions as a partial condenser. The condenser model solves for energy and mass balances and assumes thermodynamic equilibrium for the condensate and gas phase composition of SO_2 and CO_2. The vapor-liquid equilibria of the gases HCl and N_2 are neglected and the components remain in the gas phase. The dissolved gases are modelled as a separate dissolved gases flow, but neglected in the re-evaporated condensate. The liquid phase concentrations of CO_2 and SO_2 are calculated according to Henry´s law (Eq. (7)), the Henry´s law constants are taken from [44]. The concentration of water in the gas phase is calculated according to saturation vapor pressure (Eq. (8)), which uses the IAPWS-IF97 formulation [35].

$$y_{CO_2/SO_2,dry\ FG} \cdot p_{condenser} = x_{CO_2/SO_2,condensate} \cdot \frac{1}{H_{CO_2/SO_2,water}} \tag{7}$$

$$p_{condenser} \cdot y_{H_2O,dry\ FG} = p_s(t_{condenser}) \tag{8}$$

Several simulation cases are evaluated, considering the O_2 concentration in the steam/O_2-mixture, the temperatures in the fluidized bed and freeboard, and the injection of liquid condensate into the freeboard. Depending on the case, these quantities are either prescribed as input parameters or determined as resulting variables. In each simulation, all not varied parameters are set to a design case. Table 1 summarizes the main model parameters and design case parameters for the oxy-steam process.

Table 1. *Overview of the model parameters*

Parameter	Range	Design case
Rated thermal input	6 MW	-
Fuel (water content, ash content)	Wood, tomato crop waste	Wood
Biomass water content	Wood: 0.05-0.5 kg/kg_{tot}, crop waste: 0.5-0.6 kg/kg_{tot}	0.4 kg/kg_{tot}
Biomass ash content	Wood: 0.003 kg/kg_{dry}, crop waste: 0.1871 kg/kg_{dry}	0.003 kg/kg_{dry}
Primary oxygen-excess ratio	0.6 - 1	0.7
Global oxygen-excess ratio	1	-
Heating network return temperature	20-70 °C	40 °C
Heating network supply temperature	70-100 °C	70 °C
Pinch temperature difference in partial condenser	10 K	-
Heat losses of the boiler	1 % of rated thermal input	-
O_2 concentration in the steam/O_2-mixture	10-25 mol%	15 mol%
Pressure loss	Fluidized bed: 0.2 bar, other: 0 bar	-
Main steam parameters	5 bar, 160 °C	-
Pump and fan efficiency	$\eta_{s,pump} = 0.7$, $\eta_{s,fan} = 0.85$, $\eta_{mech} = 0.9$	-

To compare the oxy-steam process with air combustion and conventional oxyfuel combustion with wet and dry FGR, simulation models of those processes are also setup in IPSEpro. Figure 2 shows the simplified model structure of these cases. The design case parameters of Table 1 are applied for process comparison.

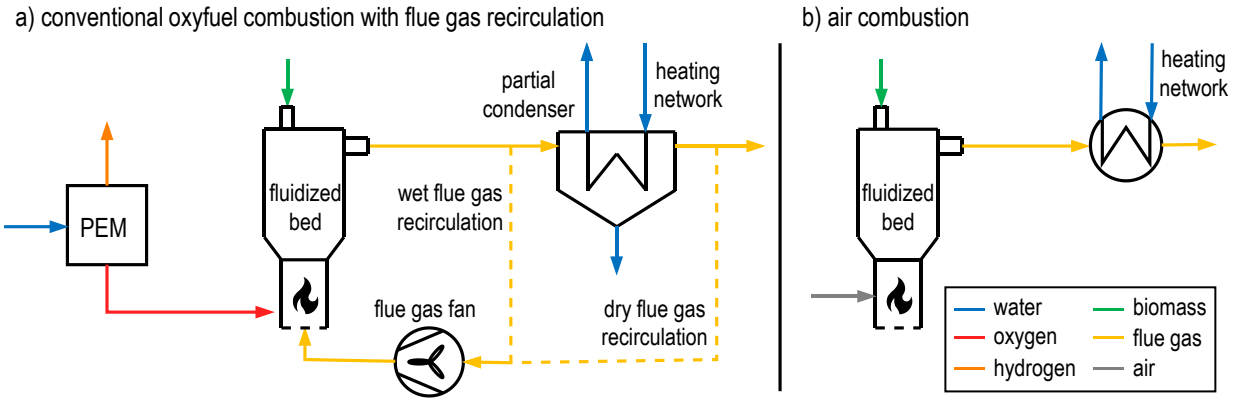

Figure 2. *Simplified simulation model setup of a) conventional oxyfuel combustion with wet and dry flue gas recirculation and b) air combustion.*

3. Results of the Thermodynamic Process Simulations

For the oxy-steam combustion process (Figure 1), three approaches for cooling of the fluidized bed combustor are analyzed. First, cooling can be achieved by using biomass fuels with high moisture content. Due to the intense mixing in the fluidized bed, fuel drying and thermochemical conversion occur simultaneously, allowing cooling through the latent heat of moisture evaporation. Another option is condensate recirculation in liquid form. Similar to moist fuels, the evaporation heat of water can be utilized for cooling. However, direct injection of liquid condensate into the fluidized bed may be difficult in practice, as integrating injection nozzles into the refractory lining could be challenging. In addition, rapid evaporation may damage the refractory lining, and the injection may affect the fluidization behavior. Therefore, in a first step, only the freeboard cooling by liquid condensate injection is considered, as this cooling method is already applied in industrial fluidized bed systems [45]. Additionally, temperature control in the fluidized bed can be achieved through staged combustion [40]. The third approach involves condensate recirculation as reevaporated steam using the heat of the flue gas cooler. Steam has a significantly higher specific heat capacity than nitrogen and carbon dioxide, at 200 °C it is roughly twice as high. In contrast, the molar heat capacity of CO_2 at 200 °C is higher than that of H_2O, while nitrogen has the lowest value [46]. In fluidized bed reactors, the recirculation of steam and fluidization with a steam/O_2-mixture also ensures proper fluidization. Moreover, the mixing of steam and oxygen prevents local overheating, which could still occur when applying the other cooling methods while fluidizing with pure oxygen. For this reason, each simulation case used a steam/O_2-mixture for fluidization and temperature moderation.

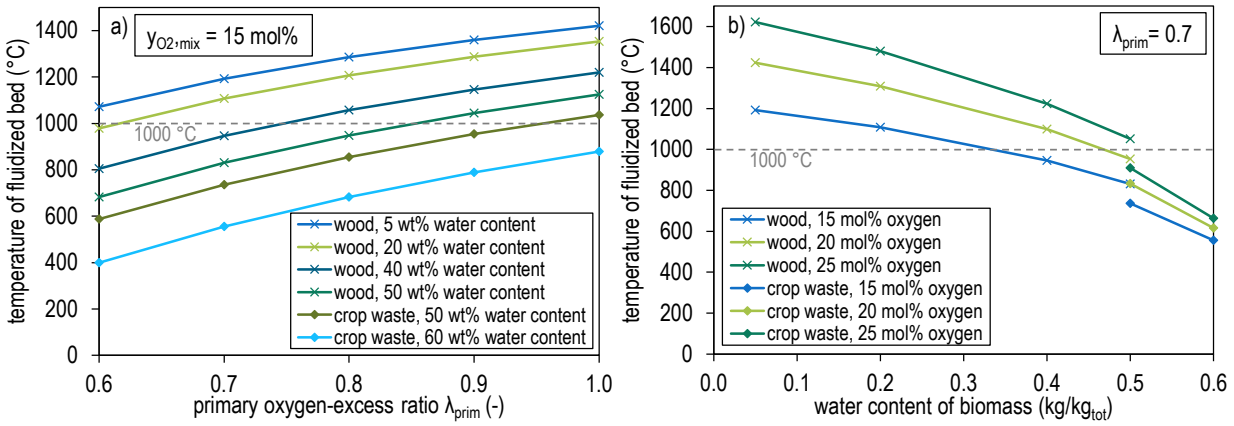

Figure 3*. Fluidized bed temperature for different fuels at a) varying primary oxygen ratios and b) oxygen concentrations in the steam/O_2 mixture.*

Figure 3 presents the fluidized bed temperature for wood and tomato crop waste at varying water contents, primary oxygen-excess ratios λ_{prim} and O_2 concentrations in the steam/O_2-mixture $y_{O_2,mix}$. Staged combustion, which results in incomplete combustion in the fluidized bed, and moist fuels allow the temperature to remain below 1000 °C, which is selected as a limit to prevent ash melting. At $\lambda_{prim} = 0.7$ and 60 wt% water content, the temperature reaches only 555 °C. Increasing the O_2 concentration in the steam/O_2-mixture from 15 to 25 mol% raises the temperature to 663 °C.

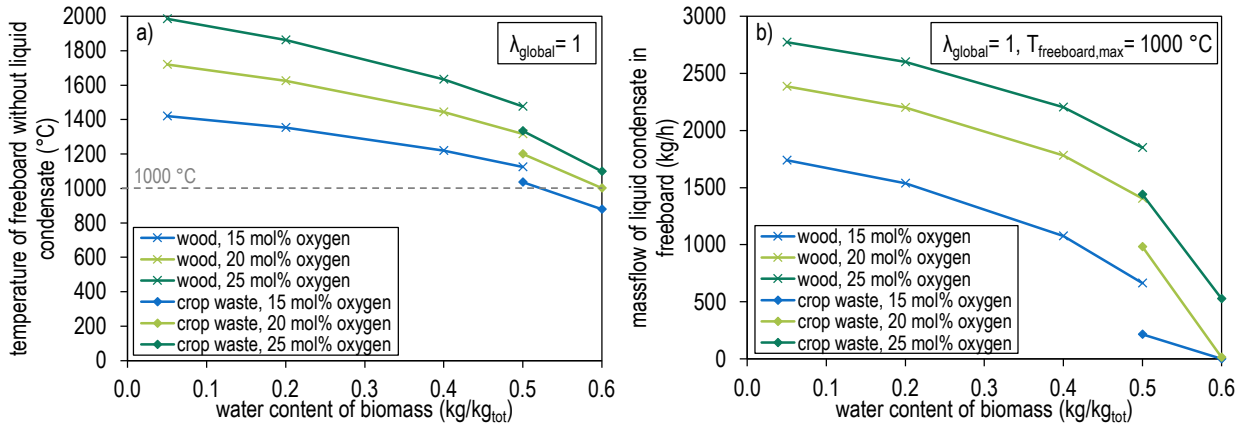

Figure 4. *a) freeboard temperature without liquid condensate injection and b) required liquid condensate mass flow for limiting the freeboard temperature to 1000 °C.*

In the freeboard, liquid condensate is added alongside the steam/O_2-mixture to maintain temperatures below 1000 °C. Figure 4 shows the freeboard temperatures without condensate injection and corresponding condensate amount required for cooling. The condensate mass flow is set to 0 kg/h for temperatures below 1000 °C. Only crop waste with 50-60 wt% water content requires no liquid condensate for temperature control.

The thermal efficiency, calculated with Eq. (9), is based on the fuels' lower heating value and can exceed 100 % due to latent heat recovery by flue gas condensation. With flue gas condensation, the thermal efficiency increases for fuels with higher water and ash contents (Figure 5). The temperature of the dry flue gas equals the condenser temperature, which is linked to the return temperature of a heating network with a fixed pinch temperature difference of 10 K. Lower return temperatures reduce the water content of the dry flue gas and by this, increase the latent heat recovery and CO_2 concentration in the dry flue gas $y_{CO_2,\text{dry FG}}$.

$$\eta_{\text{thermal}} = \frac{\dot{Q}_{\text{heating network}}}{\dot{m}_{\text{biomass}} \cdot \text{LHV}_{\text{biomass}} + P_{\text{el,pump/fan}}} \tag{9}$$

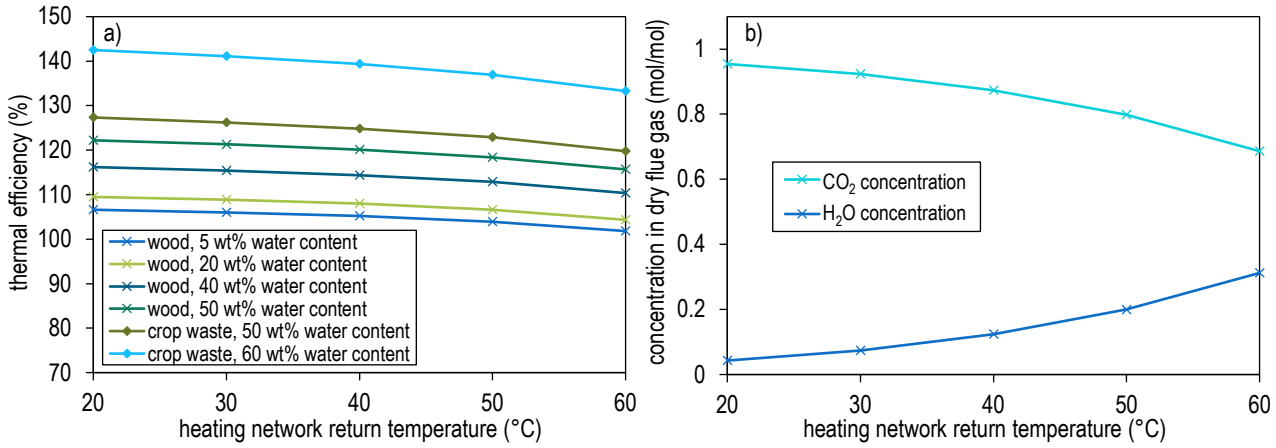

Figure 5. *a) thermal efficiency for different fuels and b) dry flue gas composition after the partial condenser for varying heating network return temperatures.*

Oxy-steam combustion with condensate recirculation is compared to conventional oxyfuel combustion with wet and dry FGR, and to air combustion without flue gas condensation applying the models in Figure 2. Unlike the previous simulations, the O_2 concentration steam/O_2-mixture is not fixed, only the temperature was fixed to 1000 °C. Wood is used as fuel. For the conventional oxyfuel combustion, staged combustion is not considered. In oxy-steam combustion staged combustion according the design case is applied to account for liquid condensate injection in the freeboard, and temperature in the fluidized bed is set to 900 °C. For air combustion, the temperature is also set to 1000 °C resulting in oxygen-excess ratios between 1.8 to 2.5. The thermal efficiencies of each oxyfuel combustion technology are very similar and due to the latent heat recovery by flue gas condensation and lower flue gas losses higher than that of air combustion (Figure 6a). At 40 wt% water content, air combustion reaches a thermal efficiency of 84 %, while oxyfuel combustion achieves

approximately 120 %. Replacing the flue gas fan with a pump in oxy-steam combustion reduces the electrical power demand from 110 kW (wet FGR) and 61 kW (dry FGR) to 1.2 kW at 40 wt% biomass water content. The molar O_2 concentration in the flue gas/O_2-mixture in dry FGR exceeds those of wet FGR as the wet flue gas is recirculated a higher temperature (180 °C) compared to dry flue gas (50 °C). This results in higher recirculating volume flows which increases the electrical pump power. Higher biomass moisture leads to stronger cooling of the fluidized bed, resulting in higher O_2 concentrations in the primary mixture. In oxy-steam combustion, freeboard cooling must therefore increasingly be provided by the injection of liquid condensate.

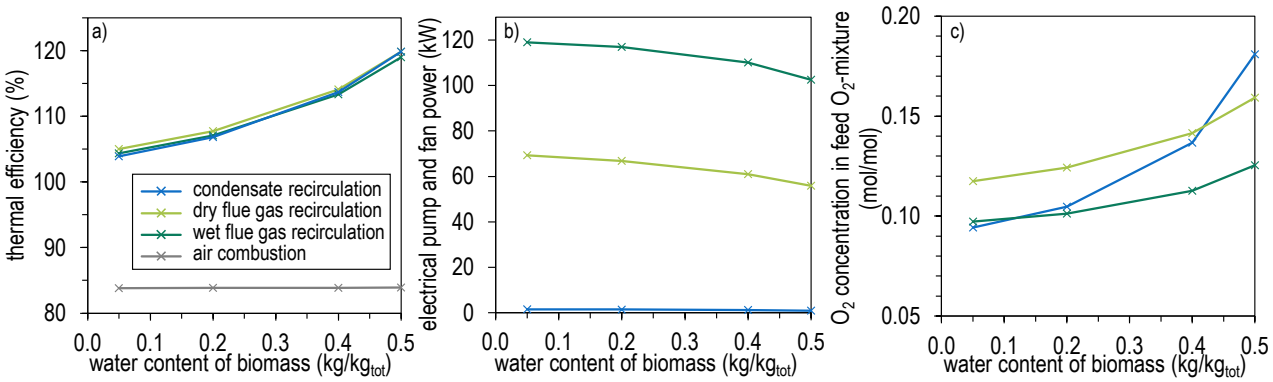

***Figure 6**. a) thermal efficiency, b) electrical pump and fan power and c) O_2 concentration in the feed O_2-mixture for different oxyfuel combustion technologies and air combustion.*

In addition to the electrical power demand, recirculating liquid condensate with subsequent evaporation of a partial stream allows a significant reduction in the pipe cross-sections required for recirculation. The specific volume of liquid water (0.0010 m^3/kg) is much lower than that of the dry recirculated flue gas (0.68 m^3/kg). Maintaining typical flow velocity limits (1 m/s for liquids and 15 m/s for flue gas and steam [47]) allows the pipe cross-sections to be reduced by roughly a factor of 9. In addition, since evaporation takes place at a higher pressure level than the flue gas recirculation, the pipe cross-sections in this section of the plant can also be reduced by approximately a factor of 2.

4. Experimental Setup of the Process Chain

The process chain of an air-operated bubbling fluidized bed reactor is expanded for oxy-steam combustion and designed for a thermal input of 10-20 kW_{th}. Figure 7 shows a simplified R&I scheme of the experimental setup. The BFB reactor (Figure 8a) has a modular structure that allows for different fluidized bed and freeboard heights. The fluidized bed section has a diameter of 200 mm, expanding to 400 mm in the freeboard section. A screw feeder supplies biomass from above via the cover. The primary mixture (air or steam/O_2) enters the reactor through a porous plate at the bottom. The fluidized bed can be preheated with an 9 kW electrical heater, and the primary air can be preheated up to 400 °C with an electrical flow heater [48]. The secondary mixture enters the reactor tangentially above the fluidized bed section.

For oxy-steam operation, oxygen is supplied from gas bottles and controlled by a mass flow controller. A steam generator provides saturated steam at 7 bar_{abs}, which is controlled with a Coriolis mass flow meter and control valve. The process chain is designed so that no pure oxygen enters the fluidized bed to avoid the safety risk of too high temperatures. Therefore, a mixing chamber gently and efficiently mixes the two streams (Figure 8b). Oxygen is supplied from the top and steam is supplied tangentially from the side to create turbulence. The oxygen entrance is positioned below the steam/O_2 outlet to prevent oxygen from bypassing. The mixing chamber also serves as a condensate drain. After the mixing chamber, the mixture splits into a primary and secondary flow, enabling staged combustion in oxy-steam operation as well. This split is achieved using a control valve and a Coriolis mass flow meter.

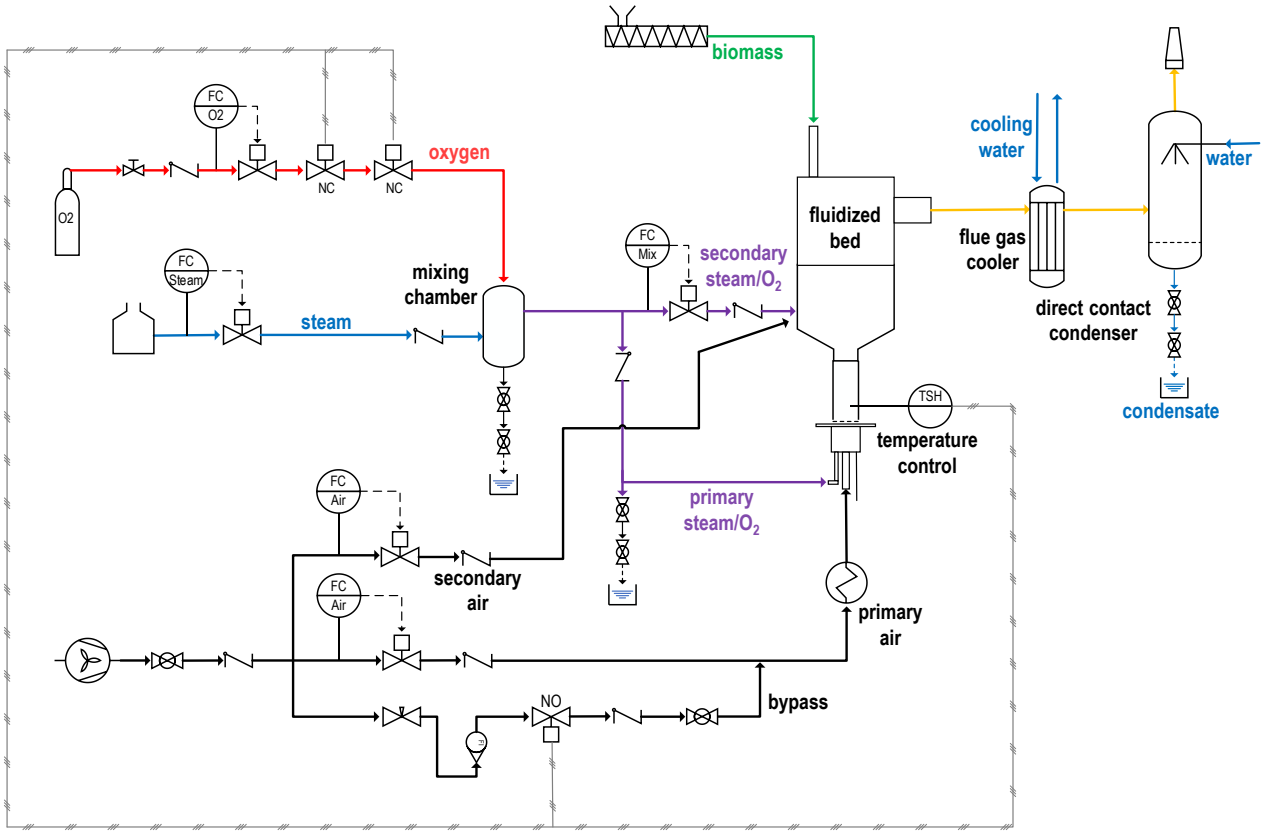

Figure 7. *Simplified R&I scheme of the oxy-steam fluidized bed combustion experimental setup.*

In the fluidized bed, temperature control limits the temperature to 900 °C. When the temperature control is triggered, the emergency stop activates. The normally closed (NC) valves in the oxygen line switch off, interrupting the heating and the fuel supply. In addition, the air bypass opens to maintain fluidization and ensure the complete oxidation of the remaining fuel in the reactor. This prevents the formation of explosive mixtures due to incomplete combustion.

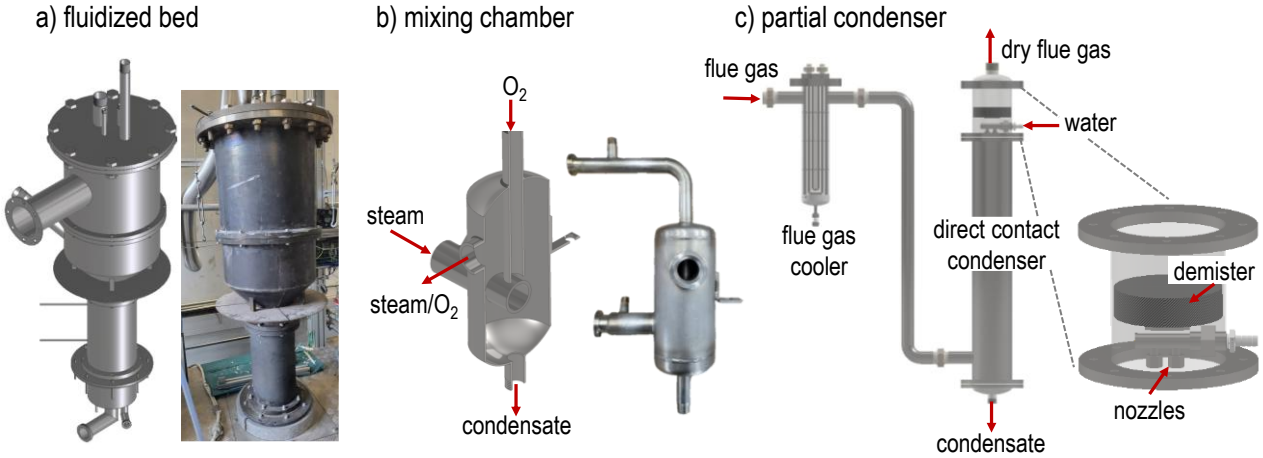

Figure 8. *a) CAD model and photo of the lab-scale fluidized bed without thermal insulation, b) CAD model and photo of the mixing chamber [49] and c) CAD model of the partial condenser including flue gas cooler and direct contact condenser.*

In the downstream process, a partial condenser is integrated to produce a CO_2-rich flue gas stream. The flue gas cooling is separated from the condensation step reflecting industrial practice where the hot flue gas is first cooled by steam generation before entering the condenser (Figure 8c). The flue gas cooler is a U-tube bundle with flue gas flowing in the shell and cooling water in the tubes. Baffles are installed on the shell side to enhance turbulence and improve heat transfer. If condensation occurs in the pre-cooler, the condensate can be removed via a drain at the bottom. For the condensation step, a direct contact condenser, as commonly applied in oxyfuel combustion systems, is selected [50]. Compared to indirect condensers, advantages include a

simple and compact setup and maintenance, higher corrosion resistance, lower pinch temperature differences and high heat exchange coefficients due to direct contact with the cooling water. In addition, the condenser can serve as a flue gas scrubber, removing sulphur and chlorine components [50–52]. One disadvantage is the water consumption, which can be avoided by recirculating the condensate as cooling medium after intercooling it [53]. In the initial setup, the condenser is operated without a packing. Cooling water is distributed via nozzles and a demister prevents droplet entrainment.

5. Conclusion and Outlook

Thermodynamic process simulation evaluated the oxy-steam concept for biomass fuels, focusing on different cooling approaches: the usage of moist fuels, staged combustion combined with liquid condensate injection in the freeboard, and condensate re-evaporation to form a steam/O_2-mixture. For safe operation and stable fluidization, oxygen should always be premixed with steam. The thermal efficiency increases with decreasing condenser temperature and higher fuel moisture content. Lower condenser temperatures also lead to a higher CO_2 purity in the flue gas stream and reduce the energy demand for subsequent purification. Compared to oxyfuel systems with FGR, oxy-steam combustion achieves similar efficiency, but requires less electrical power, as the flue gas fan is replaced with a pump, and a smaller sized recirculation loop.

At a laboratory scale, an existing facility is being retrofitted for oxy-steam operation. The setup comprises a steam and oxygen supply, a mixing chamber, the BFB reactor, a flue gas cooler, and a direct contact condenser. Future work will demonstrate oxy-steam combustion with CO_2 recovery via partial condensation. Upcoming experiments will analyze the condensate to develop a recirculation concept with potential purification steps and evaluate CO_2 quality for applications such as greenhouse fertilization and PtX synthesis.

Acknowledgments

This research was funded by the German Federal Ministry for Economic Affairs and Climate Action (BMWK) within the “OxyGreenCO_2” project [funding code 03EI5480A]. Responsibility for this publication lies with the authors.

Nomenclature

A	area, m^2
F	Faraday constant, As/mol
H	Henry’s law constant, mol/(mol*bar)
i	current density, A/m^2
LHV	lower heating value, kJ/kg
$\dot{m}$	mass flow rate, kg/s
$\dot{n}$	mole flow rate, mol/s
P	power, W
$\dot{Q}$	heat flow rate, W
U	voltage, V
w	mass fraction, kg/kg
x	molar fraction in liquid phase, mol/mol
y	molar fraction in gas phase, mol/mol

Greek symbols

η	efficiency, %
λ	oxygen-excess ratio, kg/kg

Subscripts and superscripts

el	electrical
FG	flue gas
mix	steam/O_2-mixture
$mech$	mechanical
nom	nominal
$prim$	primary
s	saturation / isentropic
sec	secondary
th	thermal

References

[1] Fröhlich T, Blömer S, Münter D, Brischke L-A. CO2-Quellen für die PtX-Herstellung in Deutschland - Technologien, Umweltwirkung, Verfügbarkeit. Heidelberg; 2019. ifeu paper.

[2] Styles D, Bishop G, Ofori E, Hennig C, Bang C, Bentsen NS, Koponen K, Berndes G, Cowie A. BECCUS Science and Policy: WP7 Summary Report. IEA Bioenergy; 2025. Available at: https://www.ieabioenergy.com/blog/publications/beccus-science-and-policy/ [accessed 2026 Mar 12].

[3] Singh DV, Nagappan S, Lay C, Igliński B, Piechota G, Kumar G, Saldivar RP, Kumar V. Bioenergy carbon capture storage and utilization: a critical review of market dynamics and policy implications. 2026. p. 12. doi:10.1186/s13068-025-02724-4.

[4] Kraxner F, Nilsson S, Obersteiner M. Negative emissions from BioEnergy use, carbon capture and sequestration (BECS)—the case of biomass production by sustainable forest management from semi-natural temperate forests. 2003. p. 285–296. doi:10.1016/S0961-9534(02)00172-1. (Proceedings of the IEA Bioenergy Task 31 Workshop “Principles and Practice of Forestry and Bioenergy in Densely-Populated Regions”).

[5] Wang A, Lv J, Wang J, Shi K. CO2 enrichment in greenhouse production: Towards a sustainable approach. 2022. p. 1029901. doi:10.3389/fpls.2022.1029901.

[6] Ministry of Agriculture, Food and Agribusiness. Supplemental carbon dioxide in greenhouses. 2022. Available at: https://www.ontario.ca/page/supplemental-carbon-dioxide-greenhouses? [accessed 2026 Mar 16].

[7] Li Y, Ding Y, Li D, Miao Z. Automatic carbon dioxide enrichment strategies in the greenhouse: A review. 2018. p. 101–119. doi:10.1016/j.biosystemseng.2018.04.018.

[8] Dion L-M, Lefsrud M, Orsat V. Review of CO2 recovery methods from the exhaust gas of biomass heating systems for safe enrichment in greenhouses. 2011. p. 3422–3432. doi:10.1016/j.biombioe.2011.06.013.

[9] Ling JLJ, Yang W, Park HS, Lee HE, Lee SH. A comparative review on advanced biomass oxygen fuel combustion technologies for carbon capture and storage. 2023. p. 128566. doi:10.1016/j.energy.2023.128566.

[10] Liu Q, Shi Y, Zhong W, Yu A. Co-firing of coal and biomass in oxy-fuel fluidized bed for CO2 capture: A review of recent advances. 2019. p. 2261–2272. doi:10.1016/j.cjche.2019.07.013.

[11] Anthony EJ. Fluidized bed combustion of alternative solid fuels; status, successes and problems of the technology. 1995. p. 239–268. doi:10.1016/0360-1285(95)00005-3.

[12] Lupion M, Alvarez I, Otero P, Kuivalainen R, Lantto J, Hotta A, Hack H. 30 MWth CIUDEN Oxy-cfb Boiler - First Experiences. 2013. p. 6179–6188. doi:10.1016/j.egypro.2013.06.547.

[13] Kuhn A, Graf C, Ströhle J, Epple B. Experimental study on oxyfuel-combustion of solid recovered fuel using ilmenite as bed material in a 1 MWth fluidized bed reactor. 2025. p. 100436. doi:10.1016/j.ccst.2025.100436.

[14] Tan Y, Jia L, Wu Y. Some Combustion Characteristics of Biomass and Coal Cofiring under Oxy-Fuel Conditions in a Pilot-Scale Circulating Fluidized Combustor. 2013. p. 7000–7007. doi:10.1021/ef4011109.

[15] Romeo LM, Díez LI, Guedea I, Bolea I, Lupiáñez C, González A, Pallarés J, Teruel E. Design and operation assessment of an oxyfuel fluidized bed combustor. 2011. p. 477–484. doi:10.1016/j.expthermflusci.2010.11.011.

[16] Lupiáñez C, Mayoral MC, Guedea I, Espatolero S, Díez LI, Laguarta S, Andrés JM. Effect of co-firing on emissions and deposition during fluidized bed oxy-combustion. 2016. p. 261–268. doi:10.1016/j.fuel.2016.07.027.

[17] Kosowska-Golachowska M, Luckos A, Kijo-Kleczkowska A. Pollutant Emissions during Oxy-Fuel Combustion of Biomass in a Bench Scale CFB Combustor. 2022. p. 706. doi:10.3390/en15030706.

[18] Duan L, Duan Y, Zhao C, Anthony EJ. NO emission during co-firing coal and biomass in an oxy-fuel circulating fluidized bed combustor. 2015. p. 8–13. doi:10.1016/j.fuel.2015.01.110.

[19] Liu Q, Zhong W, Yu A, Wang C-H. Co-firing of coal and biomass under pressurized oxy-fuel combustion mode: Experimental test in a 10 kWth fluidized bed. 2022. p. 133457. doi:10.1016/j.cej.2021.133457.

[20] Sung J-H, Back S-K, Jeong B-M, Kim J-H, Choi HS, Jang H-N, Seo Y-C. Oxy-fuel co-combustion of sewage sludge and wood pellets with flue gas recirculation in a circulating fluidized bed. 2018. p. 79–85. doi:10.1016/j.fuproc.2017.12.005.

[21] Nguyen HK, Moon J-H, Jo S-H, Park SJ, Seo MW, Ra HW, Yoon S-J, Yoon S-M, Song B, Lee U, et al. Oxy-combustion characteristics as a function of oxygen concentration and biomass co-firing ratio in a 0.1 MWth circulating fluidized bed combustion test-rig. 2020. p. 117020. doi:10.1016/j.energy.2020.117020.

[22] Tondl G. Oxyfuel Verbrennung von Klärschlamm [Dissertation]. Wien: Technische Universität Wien; 2013.

[23] Sher F, Pans MA, Sun C, Snape C, Liu H. Oxy-fuel combustion study of biomass fuels in a 20 kWth fluidized bed combustor. 2018. p. 778–786. doi:10.1016/j.fuel.2017.11.039.

[24] Vodička M, Michaliková K, Hrdlička J, Hofbauer C, Winter F, Skopec P, Jeníková J. External bed materials for the oxy-fuel combustion of biomass in a bubbling fluidized bed. 2021. p. 128882. doi:10.1016/j.jclepro.2021.128882.

[25] Jin B, Zhao H, Zou C, Zheng C. Comprehensive investigation of process characteristics for oxy-steam combustion power plants. 2015. p. 92–101. doi:10.1016/j.enconman.2015.04.031.

[26] IEA Greenhouse Gas R&D Programme (IEA GHG). 2nd Meeting of the Oxy-Fuel Network. 2007. Available at: https://publications.ieaghg.org/technicalreports/2007-16%202nd%20Oxy-Fuel%20Network%20Meeting.pdf [accessed 2025 Dec 11]. Report No.: 2007–16.

[27] Seepana S, Jayanti S. Steam-moderated oxy-fuel combustion. 2010. p. 1981–1988. doi:10.1016/j.enconman.2010.02.031.

[28] Deng L, Zhao Y, Sun S, Feng D, Zhang W. Review on thermal conversion characteristics of coal in O2/H2O atmosphere. 2022. p. 107266. doi:10.1016/j.fuproc.2022.107266.

[29] Sheng L, Liu X, Si J, Xu Y, Zhou Z, Xu M. Simulation and comparative exergy analyses of oxy-steam combustion and O2/CO2 recycled combustion pulverized-coal-fired power plants. Elsevier BV; 2014. p. 267–278. doi:10.1016/j.ijggc.2014.06.011.

[30] Moroń W, Rybak W. NOx and SO2 emissions of coals, biomass and their blends under different oxy-fuel atmospheres. 2015. p. 65–71. doi:10.1016/j.atmosenv.2015.06.013.

[31] Lu P, Hao J, Yu W, Zhu X, Dai X. Effects of water vapor and Na/K additives on NO reduction through advanced biomass reburning. 2016. p. 60–66. doi:10.1016/j.fuel.2015.12.037.

[32] Escudero AI, Aznar M, Canalís P, Llera E, Díez L. Wet oxy-combustion of blends of coal and biomass. 2021. doi:10.2139/ssrn.3817253.

[33] Díez LI, García-Mariaca A, Llera-Sastresa E, Canalís P. On the oxy-combustion of blends of coal and agro-waste biomass under dry and wet conditions. 2024. p. 131265. doi:10.1016/j.fuel.2024.131265.

[34] SimTech GmbH. IPSEpro, Version 8.0. 2021.

[35] SimTech GmbH. IPSEpro Process Simulator, Process Simulation Environment: User Manual Version 8.0, 2021.03.23: R2.0. 2021.

[36] Hemetsberger S. Gasification in Power to Gas concepts - Simulation of advanced process configurations [Dissertation]. Wien: Technische Universität Wien; 2017.

[37] Carmo M, Fritz DL, Mergel J, Stolten D. A comprehensive review on PEM water electrolysis. 2013. p. 4901–4934. doi:10.1016/j.ijhydene.2013.01.151.

[38] Alkhaldi S, Aziz M, Amrite A, Prasad AK. Parametric study of PEM water electrolyzer performance. 2025. p. 327–343. doi:10.1007/s10800-024-02187-9.

[39] Buttler A, Spliethoff H. Current status of water electrolysis for energy storage, grid balancing and sector coupling via power-to-gas and power-to-liquids: A review. 2018. p. 2440–2454. doi:10.1016/j.rser.2017.09.003.

[40] Gaderer M, Gölles M, Hartmann H, Hofbauer H, Kaltschmitt M, Keil F, Nussbaumer T, Spliethoff H. Direkte thermo-chemische Umwandlung (Verbrennung). Kaltschmitt M, Hartmann H, Hofbauer H, editors. Berlin, Heidelberg: Springer; 2016.

[41] DIN EN ISO 17225-1, Biogene Festbrennstoffe Brennstoffspezifikationen und -klassen Teil 1: Allgemeine Anforderungen (ISO 17225-1:2021); Deutsche Fassung EN ISO 17225-1:2021.

[42] Callejón-Ferre AJ, Velázquez-Martí B, López-Martínez JA, Manzano-Agugliaro F. Greenhouse crop residues: Energy potential and models for the prediction of their higher heating value. 2011. p. 948–955. doi:10.1016/j.rser.2010.11.012.

[43] Baumbach G, Hartmann H, Höfer I, Hofbauer H, Hülsmann T, Kaltschmitt M, Lenz V, Neuling U, Nussbaumer T, Obernberger I, et al. Grundlagen der thermo-chemischen Umwandlung biogener Festbrennstoffe. Kaltschmitt M, Hartmann H, Hofbauer H, editors. Berlin, Heidelberg: Springer; 2016. p. 579–814. doi:10.1007/978-3-662-47438-9_11.

[44] Sanders R. Henry's Law Constants. Linstrom PJ, Mallard WG, editors. Gaithersburg MD: National Institute of Standards and Technology.

[45] Granatstein DL. Technoeconomic Assessment of Fluidized Bed Combustors as Municipal Solid Waste Incinerators: A Summary of Six Case Studies. IEA Bioenergy Task 36; 2016. Available at: https://task36.ieabioenergy.com/wp-content/uploads/sites/34/2016/06/A_Summary_of_Six_Case_Studies-2000.pdf [accessed 2026 Mar 13].

[46] Lemmon EW, Bell IH, Huber ML, McLinden MO. Thermophysical Properties of Fluid Systems. Linstrom PJ, Mallard WG, editors. Gaithersburg MD: National Institute of Standards and Technology.

[47] Franke W, Platzer B. Rohrleitungen: Grundlagen - Planung - Montage. 3rd ed. München: Carl Hanser Verlag GmbH & Co. KG; 2025. doi:10.3139/9783446483927.

[48] Müller D, Plankenbühler T, Karl J. A Methodology for Measuring the Heat Release Efficiency in Bubbling Fluidised Bed Combustors. 2020. p. 2420. doi:10.3390/en13102420.

[49] Rösch L. Umrüstung und Wiederinbetriebnahme einer 100 kW-Wirbelschicht für die Oxyfuel-Verbrennung [Master's thesis]. Nürnberg: Friedrich-Alexander-Universität Erlangen-Nürnberg; 2026.

[50] Liu D, Jin J, Gao M, Xiong Z, Stanger R, Wall T. A comparative study on the design of direct contact condenser for air and oxy-fuel combustion flue gas based on Callide Oxy-fuel Project. 2018. p. 74–84. doi:10.1016/j.ijggc.2018.05.011.

[51] Madejski P, Kuś T, Michalak P, Karch M, Subramanian N. Direct Contact Condensers: A Comprehensive Review of Experimental and Numerical Investigations on Direct-Contact Condensation. Multidisciplinary Digital Publishing Institute; 2022. p. 9312. doi:10.3390/en15249312.

[52] Verma P, Yang Z, Axelbaum RL. A direct contact cooler design for simultaneously recovering latent heat and capturing SOx and NOx from pressurized flue gas. 2022. p. 115216. doi:10.1016/j.enconman.2022.115216.

[53] Axelbaum RL. Modular Pressurized Coal Combustion for Flexible Generation. National Energy Technology Laboratory (NETL) U.S. Department of Energy (DOE); 2019. Available at: https://netl.doe.gov/sites/default/files/2020-02/Modular-Staged-Pressurized-Oxy-combustion-Power-Plant-System-Washington-University-in-St.-Louis.pdf [accessed 2026 Mar 16].